One-Pot Sequential Heck–Suzuki Synthesis of 5-Styryl-9-Hydroxy-1H-phenalen-1-ones with Tunable Optoelectronic Properties

Sven Daniel, Thomas J. J. Müller

ACES Asian Chemical Editorial Society

doi.org/10.1002/ajoc.202500621

ASIAN JOURNAL OF ORGANIC CHEMISTRY
Research Article

www.asianjoc.org

One-Pot Sequential Heck–Suzuki Synthesis of 5-Styryl-9-Hydroxy-1*H*-phenalen-1-ones with Tunable Optoelectronic Properties

Sven Daniel[a] and Thomas J. J. Müller*[a]

Dedicated to Prof. Dr. Saeed Balalaie on the occasion of his 60th birthday.

For the preparation of novel 5-styryl-substituted 9-hydroxy-1*H*-phenalen-1-ones, a sequential Pd-catalyzed Heck vinylenation–Suzuki arylation one-pot strategy was established, providing efficient access to a library of donor–acceptor chromophores. These multifunctional conjugates are characterized by a planar, highly conjugated backbone extended through vinyl substitution at the 5-position. The obtained compounds were comprehensively investigated with respect to their electrochemical and photophysical properties. Cyclic voltammetry demonstrates that the reduction potentials remain largely unaffected by substituents, whereas the oxidation potentials show a pronounced dependence on the electronic nature of the aryl groups. UV–vis and fluorescence spectroscopy revealed bathochromic shifts of absorption and emission maxima for electron-donating substituents, while electron-withdrawing groups induce hypsochromic responses. Complementary Hammett correlations confirm the dominance of resonance effects, with the strongest linear relationships observed for the extended σ_{p+} parameter, highlighting mesomeric stabilization as the decisive factor in modulating electronic transitions. Quantum-chemical (TD)DFT calculations reproduce the spectroscopic trends and provide detailed insight into orbital contributions and charge-transfer characteristics. Solvatochromic analyses further evidence the polar nature of the excited states, supporting a pronounced intramolecular charge-transfer character.

1. Introduction

The targeted synthesis of π-conjugated donor–acceptor systems has received increasing attention in recent years,[1,2] particularly, due to their versatile potential applications in organic electronics, such as organic field-effect transistors (OFETs) and sensors,[3] organic light-emitting diodes (OLEDs),[4] and organic photovoltaics (OPVs).[5] These systems are characterized by a strong change in dipole moment upon electronic excitation due to intramolecular charge transfer between an electron-donating and an electron-withdrawing unit, which makes their optoelectronic properties particularly controllable.[6–8] Among numerous molecular acceptor moieties, 9-hydroxy-1*H*-phenalen-1-one (9-HP) has received considerable attention due to its highly electronically amphiphilic nature to form stable radical anions, radicals, and radical cations, i.e., its pronounced reversible redox activity,[9–12] and its remarkable complexing properties as a bidentate chelating ligand.[13–16] The structural peculiarity of the tricyclic 9-hydroxy-1*H*-phenalen-1-one originates from its planar, strongly conjugated structure, and its high electronic stability due to keto-enol tautomerism in conjunction with the intramolecular hydrogen bond.[17,18]

Although, functionalization of the 5-position by (hetero)aryl groups employing Suzuki cross-coupling[19] was recently achieved,[10] the introduction of other π-conjugated substituents has remained unknown to date. As a consequence of the all sp^2-hybridized, mostly strain-free ligation, in particular vinylene bridging, promises an extension of the conjugated system giving rise to planar,[20,21] electronically delocalized conjugates,[22–24] where the electronic properties can be efficiently modulated by enhanced molecular π-orbital overlap.[25,26]

At this point, palladium-catalyzed coupling processes[27] offer decisive advantages, as they are characterized by high selectivity, mild reaction conditions, and broad tolerance of functional groups. The possibility of combining palladium-catalyzed coupling processes within a multicomponent reaction (MCR) is particularly attractive. Multicomponent reactions (MCRs) represent a modern synthetic concept that offers fast and diversity-oriented access to functionalized substance libraries.[28] The reactions take place in a one-pot process, where three or more reactants are converted into a target molecule in a single reaction vessel. The process is characterized by high atom economy and significantly reduced effort in the isolation of intermediates.[29]

[a] *S. Daniel, Prof. Dr. T. J. J. Müller*
Institut für Organische Chemie und Makromolekulare Chemie, Heinrich-Heine-Universität Düsseldorf, Universitätsstraße 1, Düsseldorf D-40225, Germany
E-mail: ThomasJJ.Mueller@hhu.de

Supporting information for this article is available on the WWW under https://doi.org/10.1002/ajoc.202500621

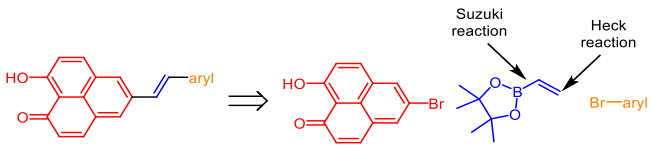

Scheme 1. Conceptional retrosynthetic analysis of 5-styryl-9-HP systems employing the one-pot Heck vinylenation-Suzuki arylation transform.

Against this background, an efficient, sequential Heck[30] vinylenation-Suzuki arylation one-pot synthesis was aimed in this work for directly and selectively accessing functionalized 9-HP derivatives with a vinylene bridge in the 5-position. Although, a vinylation with styryl derivatives could give rise to the targeted 9-HP systems, we reasoned that the aforementioned one-pot sequence represents a consecutive modular approach circumventing a preceding synthesis of styrene substrates. The electronic properties of the expected planarized targets with expanded π-conjugation were characterized in detail by cyclovoltammetry as well as UV–vis and fluorescence spectroscopy. The experimental data were subjected to Hammett correlation analysis to derive semiquantitative structure–property relationships for determining the electronic influence of the substituents. In addition, quantum chemical (TD)DFT calculations were performed to gain a deeper understanding of the underlying electronic structure of the target compounds.

2. Results and Discussion

2.1. Synthesis of 5-Styryl-substituted 9-Hydroxy-1*H*-phenalen-1-ones

Heck reaction of styryl substrates requires their preceding synthesis either from aldehydes or aryl halides. However, conceptionally a one-pot sequence consecutively ligating 5-bromo-9-HP, vinyl boronate, and aryl halides represents an alternative concise, modular approach (Scheme 1). In addition, a sequential Pd-catalyzed Heck vinylenation-Suzuki arylation one-pot synthesis also promises to increase the structural diversity of 5-styryl-substituted 9-HP dyes. From a practical perspective, two consecutive palladium-catalyzed carbon–carbon forming processes in the same reaction vessel without the need to isolate intermediates increase the overall synthetic efficiency.

The bifunctional 4,4,5,5-tetramethyl-2-vinyl-1,3,2-dioxaborolane ideally represents an electron deficient alkene for Heck vinylations to give vinyl boronate products.[31,32] Prior to this work vinyl boranes have been shown to participate in Suzuki–Heck sequences[33] and vinylsilanes have been shown to be relays for Heck–Hiyama sequences.[34] In addition, Itami and coauthors showed that vinyl 2-pyrimidyl sulfides were particularly well-suited for diversity-oriented syntheses of unsymmetrically tetrasubstituted ethylenes.[35] For developing the proposed one-pot Heck vinylation-Suzuki arylation, the Heck step was first optimized with 4-bromofluorobenzene and 4,4,5,5-tetramethyl-2-vinyl-1,3,2-dioxaborolane as substrates employing ^{19}F NMR spectroscopy for monitoring the conversion (see Supporting Information, chpt. 3.1). As a favorable catalyst system and conditions, $Pd(dba)_2$ and $HP^tBu_3BF_4$ (1:2 ratio) in THF as a solvent and *N*,*N*-dicyclohexylmethylamine as a base were identified. Without isolation and in the same reaction vessel, the successfully formed aryl vinyl pinacolyl boronate was subjected to Suzuki coupling with 5-bromo-9-hydroxy-1*H*-phenalen-1-one (see Supporting Information, chpt. 3.1). The highest yields of the 5-styryl-9-HP were obtained using Cs_2CO_3 as a base in a THF/water mixture in a ratio of 3:1 (see Supporting Information, chpt. 3.1). Although the optimized sequential Pd-catalyzed Heck vinylenation-Suzuki arylation employs the same catalyst system ($Pd(dba)_2$/$HP^tBu_3BF_4$, ratio 1:2) in both steps, it turned out that higher yields of the product were obtained by adding another loading of catalyst for the second step. With these optimized conditions for the one-pot process in hand, employing aryl bromides **1**, 4,4,5,5-tetramethyl-2-vinyl-1,3,2-dioxaborolane (**2**), and 5-bromo-9-HP (**3**) as substrates, a substance library of 8 novel styryl-substituted 9-hydroxyphenalenone derivatives **4** was synthesized as orange to dark red solids with moderate to excellent yields (30%–91%) after isolation and chromatographic purification (Scheme 2).

The structures of the target compounds **4** were assigned by comprehensive NMR spectroscopy and mass spectrometry, and the molecular composition was determined by combustion analysis. The NMR spectra show single sets of signals, indicating the apparent C_s symmetry of the aromatic moieties of compounds **4a-g** at room temperature. As expected for 5-substituted 9-HP derivatives, the hydroxy-enone functionality of the 9-HP part underlies rapid intramolecular proton exchange at room temperature due to tight hydrogen bonding.[10,36] Therefore, in the NMR spectra sharp singlets between δ 15.74 and 5.99 are found for the OH proton resonances. Expectedly, the *p*-substituted aromatic derivatives (compounds **4a-g**) give the typical AA'BB' splitting pattern in the ^{1}H NMR spectra. The *trans*-configuration of the vinylene bridge was unequivocally assigned by the appearance of vicinal coupling constants of 16.4 Hz for the methine resonances at δ 7.59 and 7.72 in the spectrum of compound **4f** (R = CN). An exemplary structural assignment based upon NMR spectra was performed for compound **4b** (R = OMe) (see Supporting Information, chpt. 4.9).

2.2. Electrochemical Properties of 5-Styryl-substituted 9-Hydroxy-1*H*-phenalen-1-ones

9-Hydroxyphenalenone is characterized by a distinctly stable redox behavior as seen in cyclovoltammetric studies.[9,10,37] Noteworthy is a typical, reversible one-electron reduction, which under mild conditions leads to the formation of a remarkably persistent radical anion in the cathodic region.[37] Direct anodic oxidation is usually not accessible under normal experimental conditions. Nevertheless, earlier studies have shown that the oxidized state can also exist in the form of a radical cation, which can be stabilized by mesomeric delocalization within the π-conjugated system. Evidence was already reported in classic studies on phenalenone derivatives, where the existence of stable radical cations could be proven photometrically.[9]

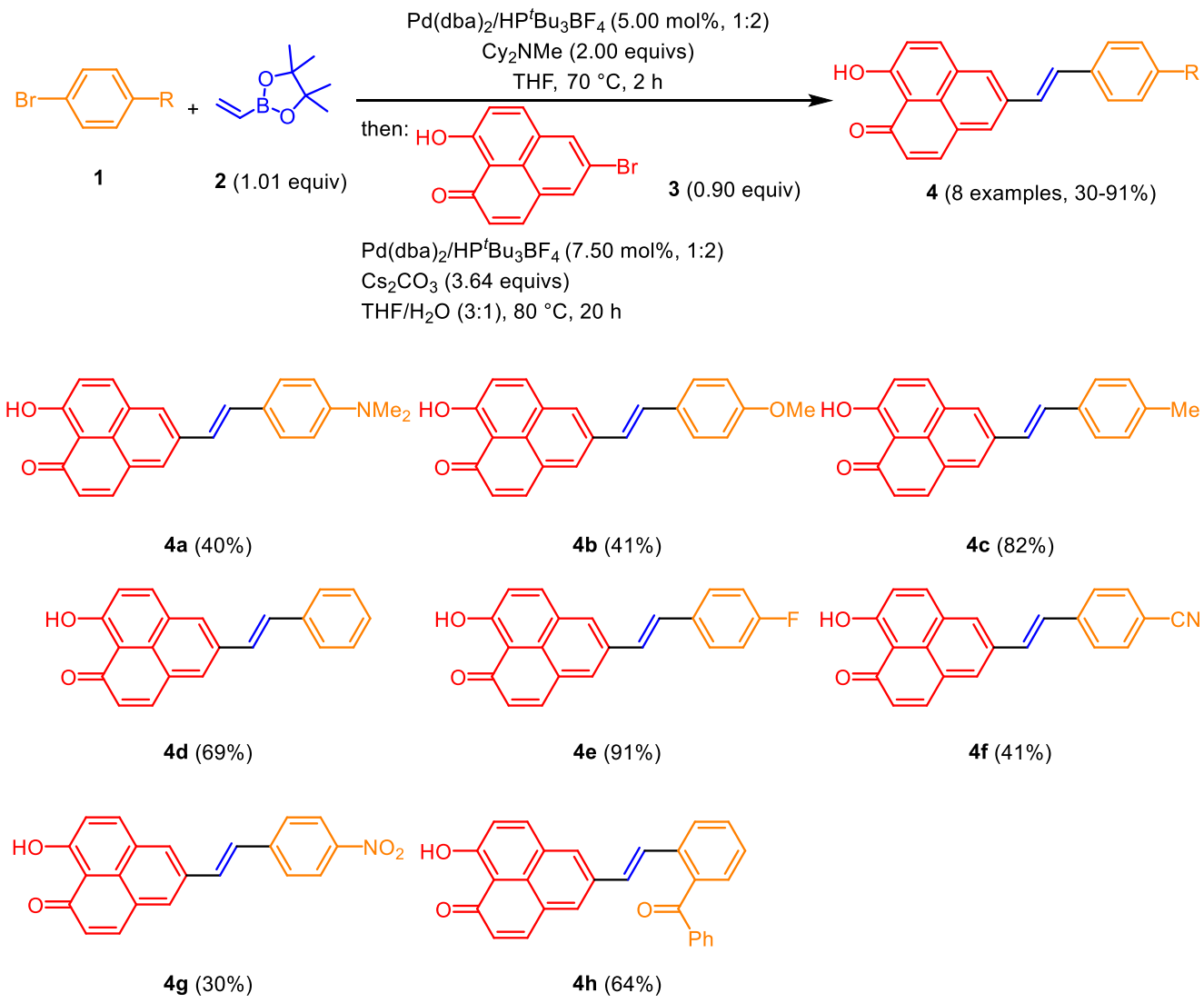

Scheme 2. One-pot Heck vinylenation-Suzuki arylation synthesis of 5-styryl-9-HP dyes **4**.

This bidirectional redox stability is unusual for a compact π-system and makes 9-hydroxyphenalenone a particularly relevant acceptor building unit in functional π-systems.

The electronic properties of the products **4** (with exception of compound **4f** due to solubility problems) were studied in the electronic ground state by cyclic voltammetry and in the excited state by UV—vis and fluorescence spectroscopy. The electrochemical properties of styryl-substituted 9-hydroxy-1*H*-phenalen-1-ones **4** were recorded in dichloromethane in the anodic and cathodic region separately (see Table 1).

The reversible reduction potentials $E_0^{0/-1}$ of all compounds investigated lie within a narrow range between −1.65 V (compound **4 h**, R = *o*-C(O)Ph) and −1.58 V (compound **4 g**, R = NO_2) (Figure 1A). Even electron-withdrawing groups such as NO_2 (**4 g**) cause only moderate anodic shifts of the reduction potential, while donor groups such as NMe_2 (**4a**) and OMe (**4b**) only slightly shift the potentials cathodically. This indicates that the electronic influence of the remote substituent on the reduction potential is only minor and, therefore, largely determined by the terminal phenalenone moiety.

In the cyclovoltammograms of compounds **4b**, **4e**, and **4h**, an additional anodic signal appears at approximately −0.2 V after several voltage cycles, suggesting the electrochemical formation of a new redox-active species. This suggests a chemical follow-up reaction of the primarily oxidized intermediate, which is either irreversible or only slowly reversible (quasi-reversible) and leads to an accumulation of an electrochemically active follow-up product in multisweep experiments. Therefore, secondary oxidations, deprotonations or structural rearrangements leading to the formation of a new type of molecule are conceivable.[39]

A comparison of the electrochemical properties of the styryl-substituted 9-hydroxy-1*H*-phenalen-1-ones presented in this work with previously investigated directly arylated derivatives[10] reveals that reduction potentials differ only marginally for identical substituents. The deviation is typically in the range of the experimental error (±0.01 V), which indicates a comparable stabilization of the radical anion and suggests that the vinylene

Table 1. Electrochemical properties of 5-styryl-substituted 9-hydroxy-1*H*-phenalen-1-ones **4**.

Compound 4[a]	R	$E_0^{0/-1}$ [V]	$E_0^{0/+1}$ [V]
4a	NMe_2	−1.64	0.14, 0.59, 0.66
4b	OMe	−1.61	0.69[b]
4c	CH_3	−1.63	0.80
4d	H	−1.61	0.91[b]
4e	F	−1.62	0.93[b],[c]
4g	NO_2	−1.58	1.01[b],[c]
4h	*o*-C(O)Ph	−1.65	0.94[b],[c]

[a] Measured in CH_2Cl_2, $T = 293$ K, electrolyte: 0.1 M NBu_4PF_6; $v = 100$ mV s^{-1}; Pt working electrode, Pt counter electrode, Ag/AgCl reference electrode, $E_0 = \frac{(E_{pa}+E_{pc})}{2}$ [V] with $[FeCp_2]/[FeCp_2]^+$ ($E_0^{0/+1} = 0.0$ V[38]) as a standard. [b] Irreversible maximum, $E_0 = \frac{(E_{p/2}+E_p)}{2}$.[39] [c] Maximum of anodic current peak.

bridge only exerts a minor influence on the electron acceptor capacity. In contrast, oxidation potentials of styryl-substituted 9-hydroxy-1*H*-phenalen-1-ones **4** of this work clearly show differences compared to the directly arylated derivatives.[10] With the exception of the directly anisyl-substituted derivative, no electrochemically detectable oxidation potentials are found for directly arylated 9-HP derivatives. The oxidation potential of compound **4b** (R = OMe) cathodically shifted by 0.4 V compared to the directly anisyl substituted 9-HP congener. Therefore, the more effective delocalization causes a better stabilization of the radical cation of **4b** and, hence, underlines the intense electronic coupling via the vinylene bridge in the electronic ground state.[22–26]

The electronic influence of the remote substituent on the electronic ground state can be semiquantitatively assessed by physical-organic structure–property relations, i.e., by Hammett correlation. Therefore, the experimentally determined half-value potentials $E_0^{0/-1}$ (reversible reduction) and $E_0^{0/+1}$ (irreversible oxidation) were plotted against various substituent-specific σ parameters, including the classic values σ_p, σ_R, and σ_I, as well as σ_{p+} and σ_{p-} (for correlation analyses, see Supporting Information, chpt. 8).[40]

For the reduction potentials, although only minor effects are seen in the cyclic voltammograms upon substituent variation, a reasonable correlation is found for the *para*-substituent parameter σ_p ($r^2 = 0.78$) (Figure 2A), directly followed by σ_{p-} ($r^2 = 0.77$) with a smaller slope, whereas σ_I gives a significantly poorer correlation ($r^2 = 0.56$) (see Supporting Information, chpt. 8). The correlation with σ_p suggests transmission of the electronic substituent effect for reduced species via inductive and mesomeric mechanisms. The poor correlations with resonance dominated stabilization (σ_R, $r^2 = 0.44$) reveals that simple mesomeric stabilization mechanisms of the radical anion are irrelevant. The resonance stabilization of discrete positive charges is a clearly poorer descriptor (σ_{p+}, $r^2 = 0.60$) than σ_{p-} ($r^2 = 0.77$), which describes stabilization of negative charges. However, for the oxidation potentials, best linear correlations are obtained upon plotting the oxidation potentials $E_0^{0/+1}$ against σ_{p+} ($r^2 = 0.89$) (Figure 2B), which accounts for a dominant contribution of mesomeric stabilization of radical cations in π-conjugated systems. The dominance of resonance stabilization is also supported for correlation with σ_R ($r^2 = 0.81$) and even for σ_p ($r^2 = 0.76$). Expectedly, correlation with σ_{p-} is very poor ($r^2 = 0.20$), as for σ_I ($r^2 = 0.13$).

2.3. Photophysical Properties of 5-Styryl-substituted 9-hydroxy-1*H*-phenalen-1-ones

All styryl-substituted 9-hydroxy-1*H*-phenalen-1-ones **4** are intensely orange to dark red solids and solutions show pronounced fluorescence under UV excitation

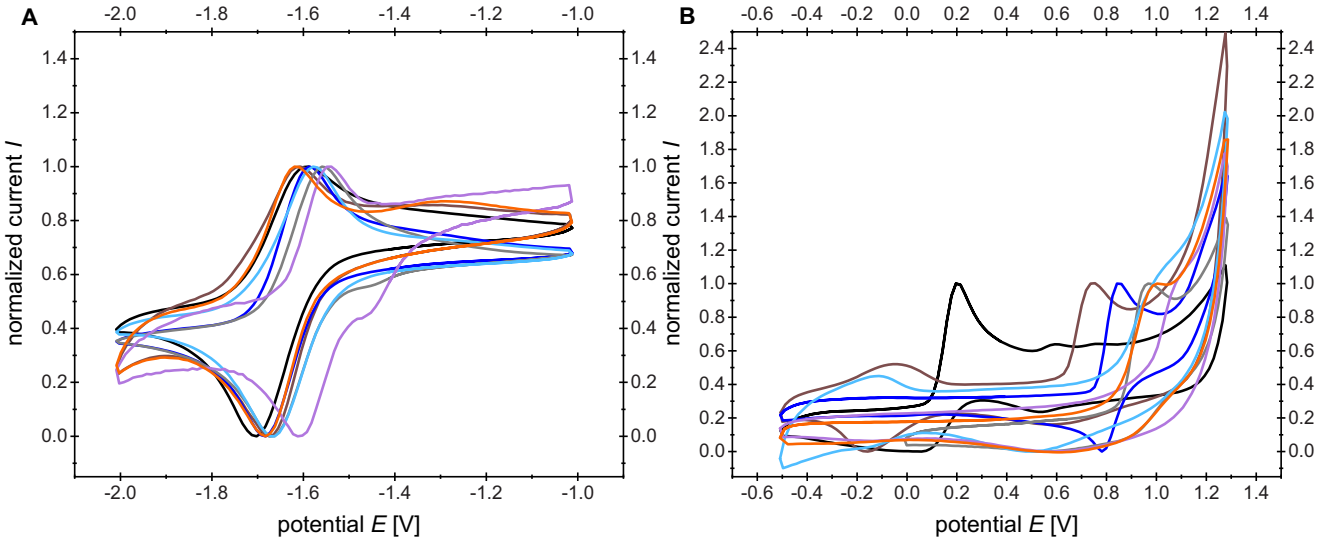

Figure 1. Normalized cyclic voltammograms of selected compounds 4 in the cathodic region (A) and compounds 4 in the anodic region (B) (measured in CH_2Cl_2, $T = 293$ K, and electrolyte: 0.1 M NBu_4PF_6; v = 100 mV s^{-1}; Pt working electrode, Pt counter electrode, and Ag/AgCl reference electrode, $[FeCp_2]/[FeCp_2]^+$ ($E_0^{0/+1} = 0.0$ V[38]) as a standard; **4a** = black, **4b** = brown, **4c** = blue, **4d** = grey, **4e** = turquoise, **4g** = violet, and **4h** = orange).

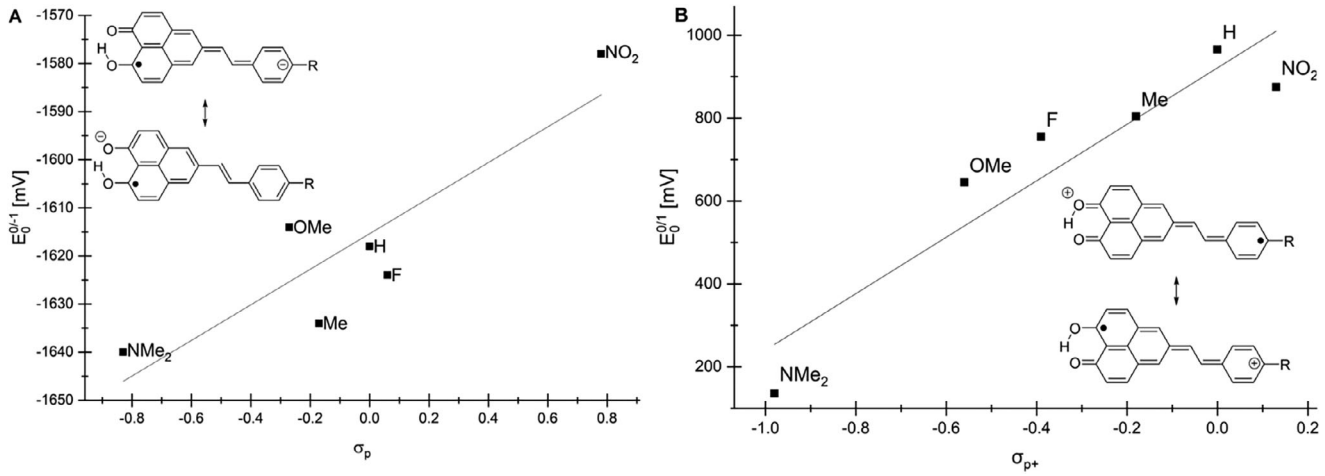

Figure 2. Hammett plots of the reduction potentials $E_0^{0/-1}$ against the substituent parameter σ_p ($E_0^{0/-1} = 36.98\ \text{mV} \cdot \sigma_p - 1615.35\ \text{mV}$; $r^2 = 0.78$) (A) and the oxidation potentials $E_0^{0/+1}$ against the substituent parameter σ_{p+} ($E_0^{0/1} = 350\ \text{mV} \cdot \sigma_{p+} + 860\ \text{mV}$; $r^2 = 0.89$) (B).

Table 2. Selected photophysical properties of styryl-substituted 9-hydroxy-1*H*-phenalen-1-ones **4**.

compound 4[a]	R	$\lambda_{max,abs}$ [nm][a] (ε [$M^{-1}cm^{-1}$])	$\lambda_{max,em}$ [nm][b] (Φ_f)[c]	$\Delta\tilde{\nu}_s$[d] [cm^{-1}]
4a	NMe_2	276 (16,800), 355 (57,600), 492 (3700)	—[e]	—
4b	OMe	331 (41,900), 350 (29,900) 466 (3600)	561 (0.15)	3600
4c	CH_3	315 (56,400), 325 (56,400), 461 (4200)	544 (0.05)	3300
4d	H	311 (28,100), 321 (28,600), 362 (sh, 6500), 455 (3000)	522 (0.14)	2800
4e	F	310 (57,800), 320 (58,400), 362 (sh, 13,800), 455 (6000)	522 (0.11)	2800
4f	CN	241 (24,300), 336 (75,000), 448 (7400)	504 (0.07)	2500
4g	NO_2	277 (12,500), 356 (21,400), 450 (3700)	500 (0.10)	2200
4h	*o*-C(O)Ph	245 (31,500), 312 (48,200), 450 (13,200)	516 (0.10)	2800

[a] Recorded in CH_2Cl_2, RT, $c(\mathbf{4}) = 10^{-5}$ M. [b] Recorded in CH_2Cl_2, RT, $c(\mathbf{4}) = 10^{-6}$ M. [c] Absolute fluorescence quantum yield measured in CH_2Cl_2, 20 °C, $c(\mathbf{4}) = 10^{-6}$ M. [d] $\Delta\tilde{\nu}_s = \frac{1}{\lambda_{max,\ abs}} - \frac{1}{\lambda_{max,\ em}}$ [in cm^{-1}]. [e] No emission detectable.

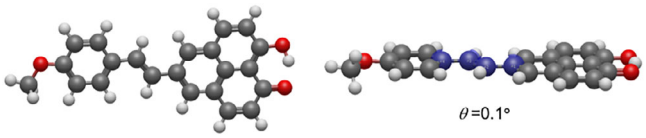

Figure 3. Optimized ground state and torsions angle θ of compound **4b** using the polarizable continuum model (PCM) with dichloromethane as solvent (Gaussian 16, B3LYP/6–31G*, PCM CH_2Cl_2).

and were investigated using UV–vis and fluorescence spectroscopy (Table 2). The emission spectra were recorded in dichloromethane at room temperature. The dyes were excited at the respective longest-wavelength absorption maximum.

The 5-styryl-substituted 9-hydroxy-1*H*-phenalen-1-ones **4** are characterized by an almost planar molecular geometry (Figure 3), as evidenced by the dihedral angle between the aromatic substituent, the vinylene bridge and the central phenalenone core. According to DFT calculations, the torsion angle characteristic of this conjugation plane is only $\theta = 0.1$ ° in the optimized S_0 state (electronic ground state), which indicates excellent coplanarity of the π-systems.[22–26] This geometric arrangement promotes efficient conjugative delocalization across the entire donor–π–acceptor system and thus forms the structural basis for pronounced intramolecular charge transfer properties.

In contrast, the directly 5-aryl-substituted 9-hydroxyphenalenones exhibit significantly higher dihedral angles.[10] For example, a torsion angle of 38 ° was determined for those systems, indicating a significant twist between the aryl residue and the phenalenone core. This geometry significantly restricts the π-conjugation between the aromatic fragments and consequently reduces the electronic coupling in the excited state. The nearly planar conformation of the vinylene-aryl systems presented here therefore represents a decisive structural advantage over the directly linked systems and explains the more intense charge transfer bands and better optoelectronic properties.

The absorption spectra of 5-styryl-substituted 9-hydroxy-1*H*-phenalen-1-ones **4** show a characteristic behavior (Figure 4A). All compounds exhibit three main absorption maxima at 300, 330, and 450 nm, where the bands around 330 nm are most intense (28,000 to 75,000 $M^{-1}cm^{-1}$). These absorption bands can be assigned to π-π* transitions of the phenalenone backbone.[10]

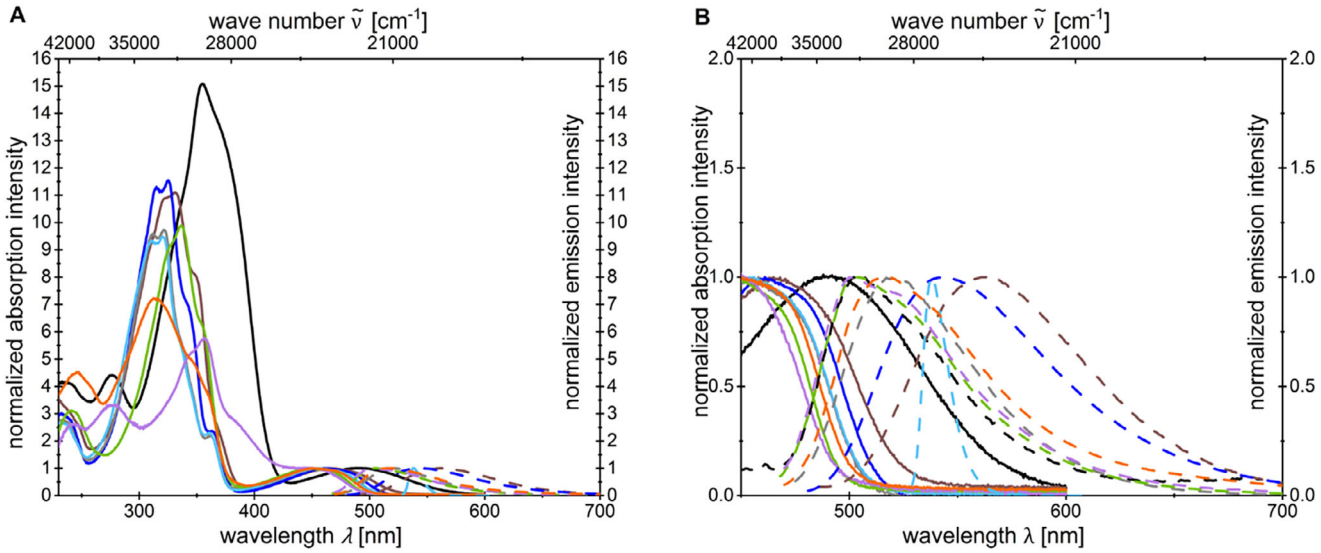

Figure 4. Comparison of the UV–vis absorption and emission spectra (A) and enlargement of the comparison of the UV–vis absorption and emission spectra (B) of the 5-styryl-substituted 9-hydroxy-1*H*-phenalen-1-ones **4** (absorption spectra measured in CH_2Cl_2, $T = 298$ K, $c(\mathbf{4}) = 10^{-5}$ M (solid lines) and emission spectra recorded in CH_2Cl_2, $T = 298$ K, $c(\mathbf{4}) = 10^{-6}$ M (dashed lines); **4a** = black, **4b** = brown, **4c** = blue, **4d** = gray, **4e** = turquoise, **4f** = green **4g** = violet, and **4h** = orange).

The longest wavelength absorption maxima are located in the range from 448 to 492 nm. These lowest energy absorption bands are lower in intensity with still significant extinction coefficients (approx. 3000–13,000 $M^{-1}cm^{-1}$). Electron-donating substituents such as the dimethylamino group (**4a**) lead to a strong bathochromic shift (492 nm), which becomes smaller with diminishing electron-releasing character (**4b**, R = methoxy, 466 nm; **4c**, R = methyl, 461 nm), compared to the unsubstituted compound **4d** (R = H, 455 nm) as a reference. Acceptor substituents such as fluorine (**4e**, 455 nm), cyano (**4f**, 448 nm), nitro (**4g**, 450 nm), and *ortho*-benzoyl (**4 h**, 450 nm) cause hypsochromic shifts compared the absorption band of compound **4d**. The red shift of the longest wavelength absorption maximum with steadily increasing donor character is in good agreement with the overall electron-withdrawing effect of the 9-hydroxy-1*H*-phenalen-1-one moiety.

The emission maxima of most of the dyes **4** appear in the range between 500 and 560 nm with emission colors in the range from yellow to orange-red (Figure 4B). Compound **4a** (R = NMe_2), however, represents a special case. Under the measurement conditions, almost no or only an extremely low emission can be detected. The calculated Stokes shifts are relatively narrow, ranging from 2100 to 3600 cm^{-1}, suggesting moderate polarization or structural rearrangement of the molecules in the excited state. Compared to other push–pull-substituted stilbenes, for which significantly larger Stokes shifts are observed,[41,42] the shifts measured here remain within the smaller range. Although electronic changes in the excited state of 5-styryl-substituted 9-hydroxy-1*H*-phenalen-1-ones **4** show typical donor–acceptor behavior, the charge-transfer characteristics are not as pronounced as for typical donor–acceptor-substituted stilbenes (dimethylamino donor, nitro acceptor). With increasing acceptor character, the Stokes shifts decrease (**4g**, R = nitro, emission at 500 nm, Stokes shift of 2200 cm^{-1}). Therefore, particularly electron-rich substituents such as the methoxy group (**4b**) exhibit a strong red-shifted emission (561 nm) as well as a simultaneously high quantum yield (15%) and the largest Stokes shift in the series (3600 cm^{-1}).

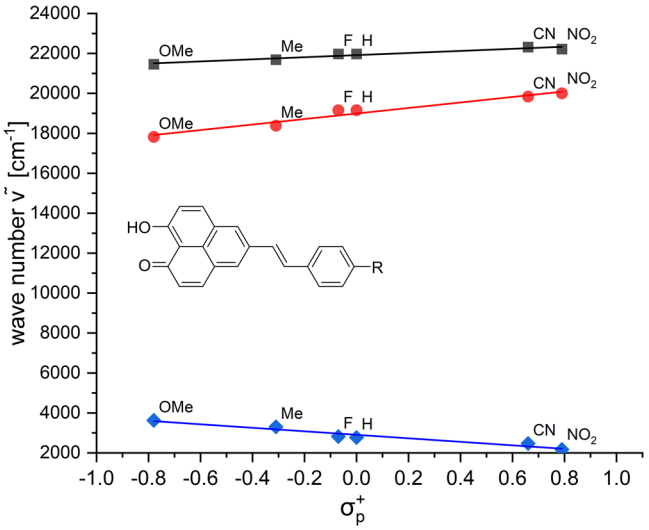

Figure 5. Linear correlation plots of the absorption ($\lambda_{max,abs}$ [nm], black), emission maxima ($\lambda_{max,em}$ [nm], red), and Stokes shifts ($\Delta\tilde{\nu}_s$ [cm^{-1}], blue) 5-styryl-substituted 9-hydroxy-1*H*-phenalen-1-ones **4** against the Hammett parameters, σ_{p+}.

The physical-organic correlation analysis of the structure–property relationships of absorption, emission and Stokes shift was elaborated with the sigma parameters σ_p, σ_R, σ_I, etc. (Figure 5). The best correlation was established with σ_{p+}. Using compounds **4b**–**4g** (**4a** and **4h** excluded, because of their deviating emission behavior and structural peculiarity). The longest-wavelength absorption correlates best with σ_{p+} ($r^2 = 0.93$) versus σ_p (0.83), σ_R (0.70), σ_{p-} (0.72), and σ_I (0.34).

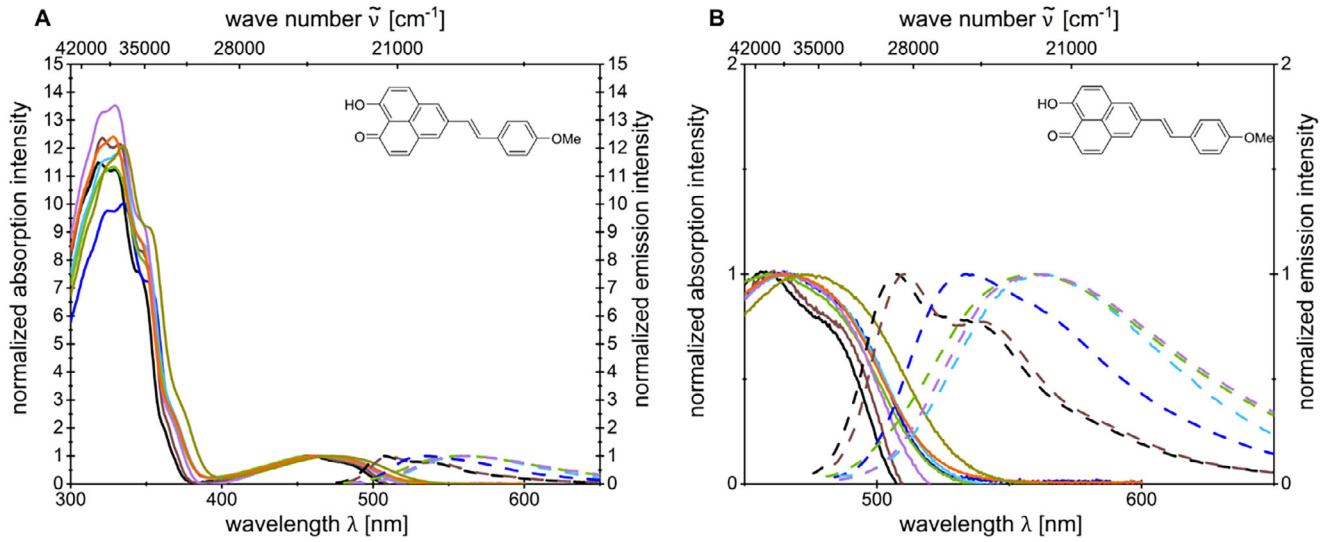

Figure 6. Normalized UV–vis absorption and emission spectra (A) and enlargement of the comparison of the UV–vis absorption and emission spectra (B) of compound 4b (absorption spectra, $T = 298$ K $c(\mathbf{4}) = 10^{-5}$ M. (solid lines)) and emission spectra ($T = 298$ K, $c(\mathbf{4}) = 10^{-6}$ M. (dashed lines)) recorded in different solvents (*n*-pentane = black, cyclohecane = brown, benzene = blue, toluene = gray, dichloromethane = turquoise, THF = green, ethyl acetate = violet, acetonitrile = orange, and DMSO = olive).

Emission maxima show the same trend with a strong σ_{p+} correlation ($r^2 = 0.96$; $\sigma_p = 0.86$; $\sigma_R = 0.70$; $\sigma_{p-} = 0.76$; $\sigma_I = 0.38$). Stokes shifts likewise scale best with σ_{p+} ($r^2 = 0.94$; $\sigma_p = 0.85$; $\sigma_R = 0.69$; $\sigma_{p-} = 0.76$; $\sigma_I = 0.38$). Collectively, mesomeric substituent effects dominate over purely inductive contributions, indicating conjugation-controlled HOMO–LUMO polarization and pronounced intramolecular CT character already in absorption and even more in the relaxed S_1 state.

The increased redshift of the emission band accounts for a highly polar excited state. Therefore, a solvatochromism study with methoxy-substituted dye **4b** was conducted to further scrutinize the highly polar excited state. In all solvents used, except DMSO and acetonitrile, the dye shows measurable emission, but with sometimes strongly varying emission maxima, quantum yields and Stokes shifts (see Supporting Information, Table S6)

The long-wave absorption maxima of the investigated derivative **4b** appear between 459 nm (*n*-pentane) and 472 nm (DMSO) (Figure 6A), which indicates a comparatively low sensitivity to solvent polarity, and thus a relatively nonpolar electronic ground state.

The emission maxima, on the other hand, vary much more significantly from 507 nm in *n*-pentane to 562 nm in ethyl acetate (Figure 6B). The pronounced bathochromic shift of the emission with increasing polarity of the solvent indicates a strongly polarized excited state (CT state).[43] It is particularly striking that the emission maxima in aromatic solvents such as benzene (534 nm) and toluene (558 nm) are already significantly red-shifted compared to nonpolar aliphatic solvents (*n*-pentane, cyclohexane), which suggests significant specific interactions, presumably π-π interactions, with aromatic solvents.

The most bathochromically shifted emission maximum and, at the same time, the largest Stokes shift is observed in ethyl acetate (562 nm; Stokes shift: 3900 cm^{-1}). The result confirms the strong electronic reorganization in the excited state and

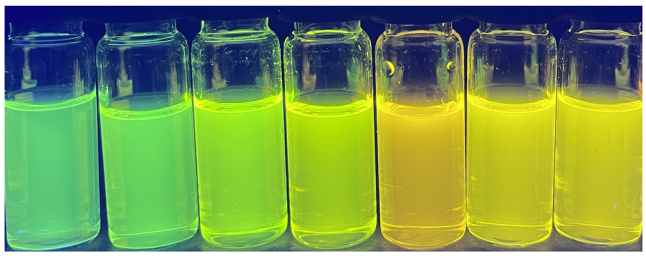

Figure 7. Emission behavior of derivative **4b** depending on solvent polarity (from left to right: *n*-pentane, cyclohexane, benzene, toluene, dichloromethane, tetrahydrofuran, and ethyl acetate; $T = 293$ K, $c(\mathbf{4}) = 10^{-6}$ M, $\lambda_{exc} = 385$ nm).

indicates a very effective stabilization of the charge transfer state by the more polar ethyl acetate. In nonpolar media such as *n*-pentane and cyclohexane, the Stokes shifts are significantly lower, with values around 2000 cm^{-1}. The strong increase in Stokes shifts from nonpolar to strongly polar solvents confirms increasing polarization in the excited state and pronounced electronic restructuring of the molecules (Figure 7).

In terms of quantum yield, *n*-pentane has the lowest value at 0.08, while medium polarities (DCM, THF, and ethyl acetate) show relatively stable values between 0.11 and 0.15. Interestingly, despite its lower polarity, benzene has a comparable quantum yield (0.14) to the medium polar solvents. No emission could be measured in the strongly polar acetonitrile and DMSO. Presumably, strong solvent-induced interactions and charge transfer processes can lead to complete extinction or low, undetectable emission.[44]

Solvatochromism was initially quantified using a Reichardt plot, in which the long-wave absorption and emission maxima were plotted as wave numbers against the $E_T(30)$[45] parameter of the solvents used (see Supporting Information, chpt. 7.1). Vibronic shoulders occur in nonpolar solvents, which is why

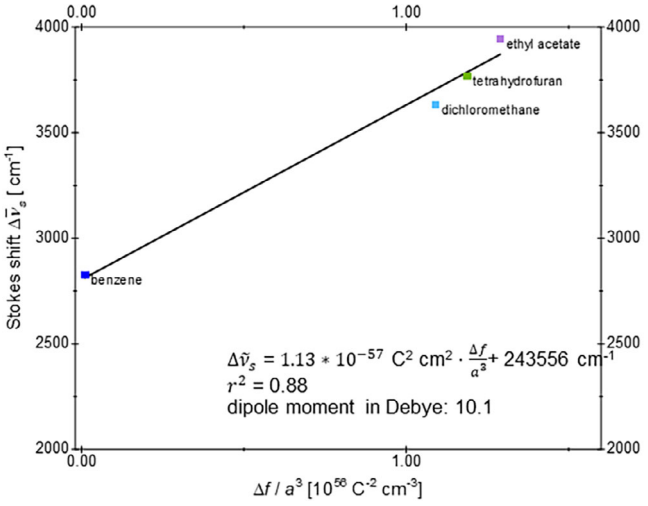

Figure 8. Correlation of the solvent-dependent Stokes shift $\Delta\tilde{\nu}_s$ (benzene, dichloromethane, tetrahydrofuran, and ethyl acetate) of derivative **4b** against the solvent-dependent factor $\Delta f/a^3$.

the Lippert–Mataga analysis was performed exclusively with polar solvents (Figure 8). The correlation of the Stokes shifts with the solvent-dependent factor $\Delta f/a^3$ allows an estimation of the dipole moment change of 10.1 Debye between S_0 and S_1, whereby the values are to be interpreted as approximations.

2.4. Calculated Electronic Structure of 5-Styryl-substituted 9-hydroxy-1*H*-phenalen-1-ones

The electronic structure of 5-styryl-substituted 9-hydroxyphenalenones **4** was elucidated by quantum chemical calculations at the (TD)DFT level of theory using the Gaussian 16 software package[46] with the density functional B3LYP[47–50] in combination with the basis set 6–31G*.[51,52] For adequately reproducing the experimentally determined absorption and emission properties in solution, the implicit polarizable continuum model (PCM) was implemented, using dichloromethane as the corresponding dielectric.[53] The TD-DFT calculations were carried out for the dyes **4** based on the optimized S_0 geometries for reproducing the absorptions and on the optimized S_1 geometries for the emission transitions (Table 3).

The calculated absorption spectra reproduce quite clearly the experimental spectra of 5-styryl-substituted 9-hydroxy-1*H*-phenalen-1-ones **4**. With exception of dye **4a**, where the longest wavelength absorption maximum is considerably underestimated in the TDDFT calculation (calcd. 622 nm versus exp. 492 nm), the deviation between calculated and experimental maxima lies in a margin from −0.06 to 0.276 eV, giving a good correlation between calculated and experimental data. As in the experimental spectra the lowest energy transitions (S_n) show a very similar pattern in the series. The unsubstituted compound **4d** (R = H) is exemplarily discussed. In the corresponding figure (Figure 9A), the calculated transitions are shown as a bar chart. The longest wavelength absorption, which represent the Franck–Condon S_1 state is dominated by a HOMO→LUMO transition, which exhibits a pronounced intramolecular charge transfer character from delocalization over the entire molecule (HOMO) to the phenalenone acceptor unit (LUMO). In addition, the HOMO–1→LUMO and HOMO–2→LUMO transitions, which correspond to the S_2 and S_4 states, also make a significant contribution and also exhibit a clear CT character. On the other hand, the HOMO→LUMO + 1 transition (S_3 state) shows as locally excited π–π^* character.

The relevant occupied and unoccupied molecular orbitals involved in these dominant electronic transitions are clearly visualized (Figure 9B). (TD)DFT calculations show that the relevant excited states are composed of precisely these orbital pairs. Comparable results were obtained for all other 5-aryl-substituted 9-hydroxy-1*H*-phenalen-1-ones **4**.

The frontier molecular orbitals (FMO) of the dyes **4a**, **4d**, and **4g** nicely illustrate the substituent effect on the FMOs (Figure 10). The HOMO energy significantly lowers from dimethylamino donor (**4a**, −0.179 eV) over electroneutral (**4d**, R = H, −0.204 eV) to nitro acceptor (**4g**, −0.215 eV). The LUMO energies, however, stay in a quite narrow range between −0.093 eV (**4a**), −0.095 eV (**4d**), and −0.101 eV (**4g**). The coefficient densities of the HOMOs are almost equally distributed across the entire molecule. In contrast, the coefficients of the LUMO orbitals are differently localized depending on the electronic nature of the substituent. Although the coefficients are mainly concentrated on the phenalenone core in donor-substituted derivatives (e.g., **4a**), they shift increasingly to the phenyl substituent in more strongly acceptor-substituted compounds (such as **4 g**). Consequently, with increasing donor strength of the substituents, photonic excitation (HOMO→LUMO) causes an increased charge transfer (CT) from the aryl substituent to the phenalenone core. The calculations reproduce self-consistently the electronic redistribution in the excited state and confirm the pronounced CT character of both longest wavelength absorption bands and shortest wavelength emission bands.

3. Conclusion

A library of 1-(9-hydroxy-1*H*-phenalen-1-one)-2-aryl ethenes, i.e., 5-styryl-9-HP dyes conjugates were synthesized by a consecutive Pd-catalyzed Heck vinylation-Suzuki arylation sequence in a one-pot fashion starting from 5-bromo-9-HP, vinyl pinacolborane, and aryl halides. This modular synthesis easily allows introducing aryl substituents ranging from electron-rich over electroneutral to electron-poor. The obtained conjugates with extended π-conjugation reveal interesting electronic properties, both in the electronic ground (as supported by cyclic voltammetry) and in the excited state (absorption and emission characteristics). Correlation analyses of the obtained reduction and oxidation potentials as well as absorption and emission bands and Stokes shifts indicate that all systems are significantly delocalized in the electronic ground and excited states with a clearly polar excited state as seen from positive emission solvatochromism. The substituent effect is mainly governed by mesomeric stabilization reflected in high σ_{p+} correlations, while inductive contributions

Table 3. Quantum chemical calculation data of 5-styryl-substituted 9-hydroxy-1*H*-phenalen-1-ones **4** (B3LYP/6–31G*).

Compound 4	R	$\lambda_{max,abs}$ (nm)[a] (ε [$M^{-1}cm^{-1}$])	$\lambda_{max,abs(cald.)}$ (nm) (oscillator strength) most dominant contribution	$\lambda_{max,em}$ (nm)[b]	$\lambda_{max,em(cald.)}$ (nm)[b](nm) (oscillator strength) most dominant contribution
4a	NMe_2	276 (16,800)	284 (0.1859) HOMO→LUMO + 3 (45%)	–[c]	740 (0.0312) HOMO→LUMO (98%)
		355 (57,600)	381 (1.5907) HOMO→LUMO + 1 (99%)		
		492 (3700)	622 (0.0404) HOMO→LUMO (98%)		
4b	OMe	331 (41,900)	335 (0.6958) HOMO-2→LUMO (81%)	561	611 (0.0443) HOMO→LUMO (98%)
		350 (29,900)	350 (1.2475) HOMO→LUMO + 1 (94%)		
		466 (3600)	520 (0.0532) HOMO→LUMO (98%)		
4c	CH_3	315 (56,400)	329 (0.8304) HOMO-2→LUMO (76%)	544	562 (0.0540) HOMO→LUMO (98%)
		325 (56,400)	342 (1.2254) HOMO→LUMO + 1 (81%)		
		461 (4200)	491 (0.609) HOMO→LUMO (98%)		
4d	H	311 (28,100)	326 (0.7097) HOMO-2→LUMO (77%)	522	542 (0.0591) HOMO → LUMO (98%)
		321 (28,600)	338 (1.2641) HOMO→LUMO + 1 (73%)		
		362 (sh, 6500)	352 (0.0312) HOMO-1→LUMO (79%)		
		455 (3000)	478 (0.0650) HOMO→LUMO (98%)		
4e	F	310 (57,800)	308 (0.0373) HOMO-5→LUMO (96%)	522	547 (0.0494) HOMO→LUMO (98%)
		320 (58,400)	327 (0.9148) HOMO-2→LUMO (72%)		
		362 (sh, 13,800)	340 (1.0622) HOMO→LUMO + 1 (64%)		
		455 (6000)	478 (0.0599) HOMO→LUMO (98%)		
4f	CN	241 (24,300)	248 (0.0782) HOMO-5→LUMO + 1 (44%)	504	506 (0.0850) HOMO→LUMO (97%)
		336 (75,000)	346 (0.9064) HOMO-1→LUMO (86%)		
		448 (7400)	454 (0.0888) HOMO→LUMO (98%)		
4g	NO_2	277 (12,500)	295 (0.4250) HOMO→LUMO + 2 (57%)	500	491 (1.1419) HOMO→LUMO (98%)
		356 (21,400)	354 (0.2786) HOMO-1→LUMO (91%)		
		450 (3700)	439 (0.8953) HOMO→LUMO (99%)		
4h	*o*-C(O)Ph	245 (31,500)	279 (0.1230) HOMO-7→LUMO + 1 (26%)	516	523 (0.0560) HOMO→LUMO (98%)
		312 (48,200)	321 (0.9715) HOMO→LUMO + 2 (38%)		
		450 (13,200)	457 (0.0692) HOMO→LUMO (97%)		

[a] Recorded in CH_2Cl_2, RT, c(**4**) = 10^{-5} M. [b] Recorded in CH_2Cl_2, RT, c(**4**) = 10^{-6} M. [c] No emissions detectable.

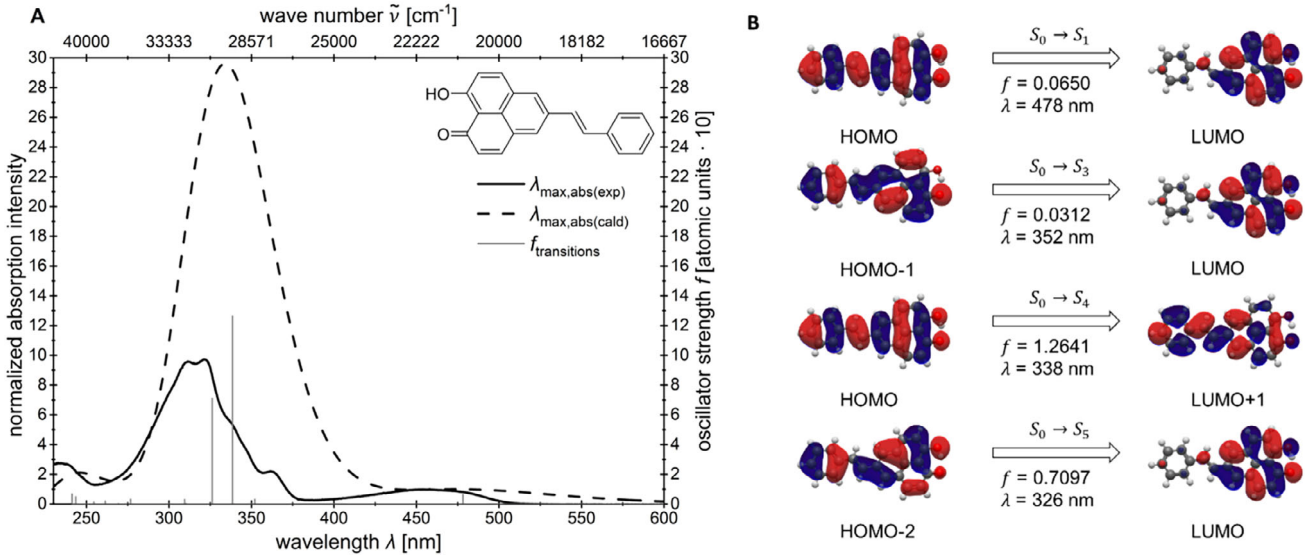

Figure 9. Comparison of the calculated (Gaussian 16, B3LYP/6–31G*, PCM CH_2Cl_2) and experimentally determined (CH_2Cl_2, T = 293 K, and c(**4**) = 10^{-5} M) UV–vis spectrum of compound **4d** with the calculated transitions (multiplied by 10) as bars (A). Calculated molecular orbitals (Gaussian 16, B3LYP/6–31G*, PCM CH_2Cl_2, isosurface value at 0.025 a.u.) of **4d** for the dominant energy transitions (B).

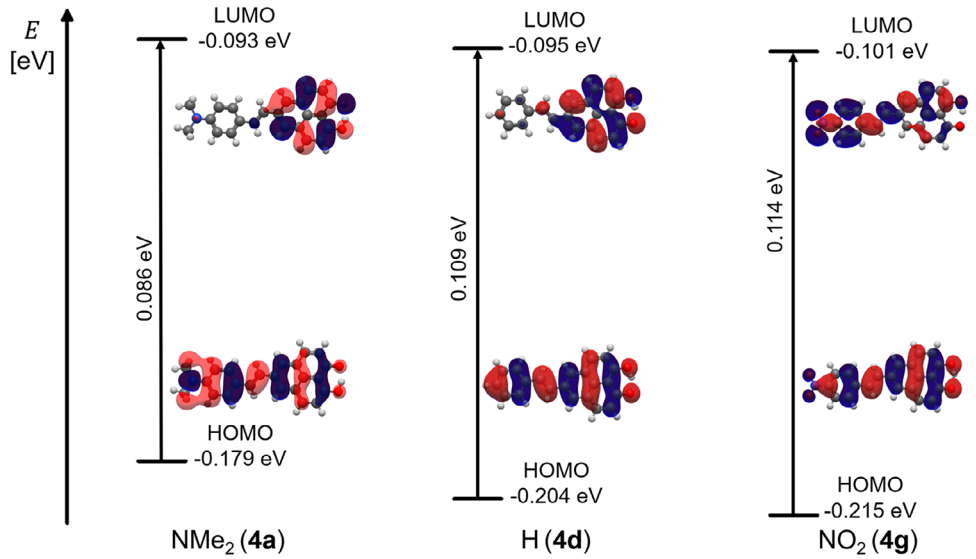

Figure 10. Selected Kohn–Sham molecular orbitals of compounds **4a**, **4d**, and **4g** using the polarizable continuum model (PCM) with dichloromethane as solvent (Gaussian 16, B3LYP/6–31G*, PCM CH_2Cl_2, isosurface value at 0.025 a.u.).

are negligible. This conjugative transmission lowers the LUMO energy of the phenalenone acceptor and amplifies the charge-transfer character, directly controlling the magnitude of the Stokes shift. The obtained fluorescence quantum yields reveal that the fluorescence emission efficiency is substantial for most systems. (TD)DFT calculations clearly support the experimentally determined properties and underline the charge transfer character of the most intensive and relevant absorptions and emissions. Particularly interesting, is that the presence of the stable intramolecular hydrogen-bonding of the carbonyl-enol moiety does not cause quenching of the emission in the excited state. The bidentate ligand nature of these expanded 9-HPs renders them interesting as ligands for square-planar noble metal complexes with tunable redox, absorption and emission properties. Studies addressing this feature are currently underway.

4. Experimental Section

4.1. One-pot Synthesis of Compound (4a) (Typical Procedure)

Under a nitrogen atmosphere, 4-bromo-*N*,*N*-dimethylaniline (**1a**) (110 mg, 0.55 mmol, and 1.00 equiv.), 4,4,5,5-tetramethyl-2-vinyl-1,3,2-dioxaborolane (**2**) (0.094 mL, 0.555 mmol, and 1.01 equiv.), palladium dibenzylideneacetone(0) (0.028 mmol, 16 mg, and 5 mol%), tri-*tert*-butylphosphonium tetrafluoroborate (0.055 mmol, 16 mg, and 10

mol%), and *N*,*N*-dicyclohexylmethylamine (0.24 mL, 1.10 mmol, and 2.00 equiv.) were dissolved in 5.50 mL dry THF and in a nitrogen-flushed Schlenk vessel. The reaction mixture was stirred at 70 °C until completion of the initial Heck vinylation was confirmed by TLC (3.5 h). The temperature was then raised to 80 °C and 9-hydroxy-1*H*-phenalen-1-one (**3**) (138 mg, 0.50 mmol, and 0.91 equiv.), Cs_2CO_3 (652 mg, 2.00 mmol, and 3.64 equiv.), additional palladium dibenzylideneacetone(0) (0.041 mmol, 24 mg, and 7.5 mol%), and tri-*tert*-butylphosphonium tetrafluoroborate (0.082 mmol, 24 mg, and 15 mol%) were added, followed by 2.5 mL dry THF and 2.7 mL distilled water. Stirring at 80 °C was continued until the Suzuki coupling was complete (20 h). After cooling to room temperature, the crude product was purified by column chromatography on silica gel (*n*-hexane/ethyl acetate 10:1) and recrystallization from acetonitrile to give compound **4a** (68 mg, 0.20 mmol, and 40%) as a dark red solid, Mp 196 °C, R_f (*n*-hexane/ethyl acetate 10:1): 0.19. ^{1}H NMR (300 MHz, $CDCl_3$): δ 3.10 (s, 6H), 6.82 (d, $^3J_{HH}$ = 9.5 Hz, 2H), 7.14 (d, $^3J_{HH}$ = 16.2 Hz, 1H), 7.23 (d, $^3J_{HH}$ = 9.3 Hz, 2H), 7.35 (d, $^3J_{HH}$ = 16.5 Hz, 1H), 7.54 (d, $^3J_{HH}$ = 9.2 Hz, 2H), 8.14 (s, 2H), 8.15 (d, $^3J_{HH}$ = 2.5 Hz, 2H), 15.90 (s, 1H). ^{13}C NMR (75 MHz, $CDCl_3$): δ 40.58 (CH_3), 111.36 (C_{quat}), 112.56 (CH), 122.84 (CH), 124.01 (CH), 125.33 (C_{quat}), 125.95 (C_{quat}), 126.05 (C_{quat}), 127.88 (CH), 130.07 (CH), 130.29 (CH), 134.73 (C_{quat}), 141.15 (CH), 150.46 (C_{quat}), 179.00 (C_{quat}). MS (EI) ((%)): 342 (23), 341 ([M]$^+$, 100), 340 (22), 326 ([M-CH_3]$^+$, 12), 297 ([M-C_2H_6N]$^+$, 15), 134 (10). Anal. calcd. for ($C_{23}H_{19}NO_2$ [341.14]):C 80.92, H 5.61, N 4.10; Found: C 81.07, H 5.57, N 4.06.

Acknowledgments

The authors are grateful to Deutsche Forschungsgemeinschaft DFG (grant Mu 1088/9–1), and the Fonds der Chemischen Industrie for financial support. The authors also thank the CeMSA @ HHU (Center for Molecular and Structural Analytics @ Heinrich Heine University) for recording the mass spectrometric and the NMR spectroscopic data.

Open access funding enabled and organized by Projekt DEAL.

Conflict of Interests

The authors declare no conflict of interest

Data Availability Statement

The data that support the findings of this study are available in the Supporting Information of this article.

Keywords: Cross coupling · Cyclic voltammetry · Donor–acceptor systems · Fluorescence · Multicomponent reactions

[1] C. Mathur, R. Gupta, R. K. Bansal, *Chem.-Eur. J.* **2024**, *30*, e202304139,
[2] Y. Liu, Y. Wu, Y. Geng, E. Zhou, Y. Zhong, *Adv. Funct. Mater.* **2022**, *32*, 2206707,
[3] Y. Niu, Z. Qin, Y. Zhang, C. Chen, S. Liu, H. Chen, *Mater. futures.* **2023**, *2*, 042401
[4] J. Bauri, R. B. Choudhary, G. Mandal, *J. Mater. Sci.* **2021**, *56*, 18837–18866,
[5] P. G. V. Sampaio, M. O. A. González, *Int. J. Energy Res.* **2022**, *46*, 17813–17828,
[6] E. Espildora, J. L. Delgado, N. Martín, *Isr. J. Chem.* **2014**, *54*, 429–439,
[7] L. Giordano, V. V. Shvadchak, J. A. Fauerbach, E. A. Jares-Erijman, T. M. Jovin, *J. Phys. Chem. Lett.* **2012**, *3*, 1011–1016,
[8] M. Curitol, X. Ragas, S. Nonell, N. Pizarro, M. V. Encinas, P. Rojas, R. P. Zanocco, E. Lemp, G. Günther, A. L. Zanocco, *Photochem. Photobiol.* **2013**, *89*, 1327–1334,
[9] D. H. Reid, *Q. Rev. Chem. Soc.* **1965**, *19*, 274–302,
[10] L. Bensch, I. Gruber, C. Janiak, T. J. J. Müller, *5-Chem.-Eur. J.* **2017**, *23*, 10551–10558,
[11] S. K. Pal, M. E. Itkis, R. W. Reed, R. T. Oakley, A. W. Cordes, F. S. Tham, T. Siegrist, R. C. Haddon, *J. Am. Chem. Soc.* **2004**, *126*, 1478–1484,
[12] A. Pariyar, G. Vijaykumar, M. Bhunia, S. K. Dey, S. K. Singh, S. Kurungot, S. K. Mandal, *J. Am. Chem. Soc.* **2015**, *137*, 5955–5960,
[13] Y. Demura, T. Kawato, H. Kanatomi, I. Murase, *Bull. Chem. Soc. Jpn.* **1975**, *48*, 2820–2824.
[14] I. C. Paul, G. A. Sim, *Proc. Chem. Soc.* **1962**, 352.
[15] A. Mukherjee, P. P. Samuel, C. Schulzke, S. K. Mandal, *J. Chem. Soc.* **2014**, *126*, 1581–1588, https://doi.org/10.1007/s12039-014-0692-y.
[16] T. Mochida, R. Torigoe, T. Koinuma, C. Asano, T. Satou, K. Koike, T. Nikaido, *Eur. J. Inorg. Chem.* **2006**, *2006*, 558–565, https://doi.org/10.1002/ejic.200500778.
[17] A. Kovács, V. Izvekov, K. Zauer, K. Ohta, *J. Phys. Chem. A* **2001**, *105*, 5000–5009,
[18] I. Gruber, L. Bensch, T. J. J. Müller, C. Janiak, B. Dittrich, *Zeitschrift für Kristallographie – Crystalline Materials* **2020**, *235*, 225–235.
[19] F. Bellina, A. Carpita, R. Rossi, *Synth* **2004**, *2004*, 2419–2440,
[20] H. Yu, Y. Wang, H. K. Kim, X. Wu, Y. Li, Z. Yao, M. Pan, X. Zou, J. Zhang, S. Chen, D. Zhao, F. Huang, X. Lu, Z. Zhu, H. Yan, *Adv. Mater.* **2022**, *34*, 2200361,
[21] V. Joseph, K. R. J. Thomas, S. Sahoo, M. Singh, D. K. Dubey, J.-H. Jou, *ACS Omega* **2018**, *3*, 16477–16488,
[22] J. Roncali, *Chem. Rev.* **1997**, *97*, 173–206,
[23] S.-Y. Song, M. S. Jang, H.-K. Shim, D.-H. Hwang, T. Zyung, *Macromol* **1999**, *32*, 1482–1487,
[24] A. Jebnouni, M. Chemli, P. Lévêque, S. Fall, M. Majdoub, N. Leclerc, *Org. Electron.* **2018**, *56*, 96–110,
[25] S. Varghese, S. Das, *J. Phys. Chem. Lett.* **2011**, *2*, 863–873,
[26] J. Li, M. Yan, Y. Xie, Q. Qiao, *Energy Environ. Sci.* **2011**, *4*, 4276–4283,
[27] T. J. J. Müller, *Metal Catalyzed Cascade Reactions*, Springer Berlin Heidelberg,Berlin, Heidelberg, **2006**, pp. 149–205.
[28] T. Lessing, T. J. J. Müller, *Appl. Sci.* **2015**, *5*, 1803–1836.
[29] M. M. Kornet, T. J. J. Müller, *mol.* **2024**, *29*, 5265,
[30] S. Jagtap, *Catal* **2017**, *7*, 267,
[31] J. J. Molloy, C. P. Seath, M. J. West, C. McLaughlin, N. J. Fazakerley, A. R. Kennedy, D. J. Nelson, A. J. B. Watson, *J. Am. Chem. Soc.* **2018**, *140*, 126–130,
[32] Z. Liu, W. Wei, L. Xiong, Q. Feng, Y. Shi, N. Wang, L. Yu, *New J. Chem.* **2017**, *41*, 3172–3176,
[33] U. K. Das, R. Clément, C. W. Johannes, E. G. Robins, H. Jong, R. T. Baker, *Catal. Sci. Technol.* **2017**, *7*, 4599–4603,
[34] K. Itami, T. Nokami, Y. Ishimura, K. Mitsudo, T. Kamei, J.-I. Yoshida, *J. Am. Chem. Soc.* **2001**, *123*, 11577–11585,
[35] K. Itami, M. Mineno, N. Muraoka, J.-I. Yoshida, *J. Am. Chem. Soc.* **2004**, *126*, 11778–11779,
[36] B. Caes, D. Jensen, Jr., *J. Chem. Educ.* **2008**, *85*, 413,
[37] K. D. Franz, R. L. Martin, *Tetrahedron* **1978**, *34*, 2147–2151,
[38] V. V. Pavlishchuk, A. W. Addison, *Inorg. Chim. Acta* **2000**, *298*, 97–102,
[39] A. J. Bard, L. R. Faulkner, H. S. White, *Electrochemical methods: fundamentals and applications*, 3rd edition, John Wiley & Sons, Hoboken, NJ, USA, **2022**.
[40] C. Hansch, A. Leo, R. W. Taft, *Chem. Rev.* **1991**, *91*, 165–195,
[41] K. Sakthivel, F. V. Singh, *ChemistrySelect* **2024**, *9*, e202403407,
[42] C. G. Fortuna, U. Mazzucato, G. Musumarra, D. Pannacci, A. Spalletti, *J. Photochem. Photobiol. A: Chem.* **2010**, *216*, 66–72,
[43] C. J. Bender, *Chem. Soc. Rev.* **1986**, *15*, 475–502,
[44] J. R. Albani, *Structure and Dynamics of Macromolecules: Absorption and Fluorescence Studies*, Elsevier Science, Amsterdam, **2004**, pp. 141–192, https://doi.org/10.1016/B978-044451449-3/50004-6.
[45] C. Reichardt, *Chem. Rev.* **1994**, *94*, 2319–2358,

[46] M. J. Frisch, G. W. Trucks, H. B. Schlegel, G. E. Scuseria, M. A. Robb, J. R. Cheeseman, G. Scalmani, V. Barone, G. A. Petersson, H. Nakatsuji, X. Li, M. Caricato, A. V. Marenich, J. Bloino, B. G. Janesko, R. Gomperts, B. Mennucci, H. P. Hratchian, J. V. Ortiz, A. F. Izmaylov, J. L. Sonnenberg, D. Williams-Young, F. Ding, F. Lipparini, F. Egidi, J. Goings, B. Peng, A. Petrone, T. Henderson, D. Ranasinghe, V. G. Zakrzewski, J. Gao, N. Rega, G. Zheng, W. Liang, M. Hada, M. Ehara, K. Toyota, R. Fukuda, J. Hasegawa, M. Ishida, T. Nakajima, Y. Honda, O. Kitao, H. Nakai, T. Vreven, K. Throssell, J. A. Montgomery, jr., J. E. Peralta, F. Ogliaro, M. J. Bearpark, J. J. Heyd, E. N. Brothers, K. N. Kudin, V. N. Staroverov, T. A. Keith, R. Kobayashi, J. Normand, K. Raghavachari, A. P. Rendell, J. C. Burant, S. S. Iyengar, J. Tomasi, M. Cossi, J. M. Millam, M. Klene, C. Adamo, R. Cammi, J. W. Ochterski, R. L. Martin, K. Morokuma, O. Farkas, J. B. Foresman, and D. J. Fox, *Gaussian, Inc.*, Wallingford CT, **2016**.
[47] A. D. Becke, *J. Chem. Phys.* **1993**, *98*, 5648–5652,
[48] C. Lee, W. Yang, R. G. Parr, *Phys. Rev. B* **1988**, *37*, 785–789,
[49] P. J. Stephens, F. J. Devlin, C. F. Chabalowski, M. J. Frisch, *J. Phys. Chem.* **1994**, *98*, 11623–11627,
[50] S. H. Vosko, L. Wilk, M. Nusair, *Can. J. Phys.* **1980**, *58*, 1200–1211,
[51] W. J. Hehre, R. Ditchfield, J. A. Pople, *J. Chem. Phys.* **1972**, *56*, 2257–2261,
[52] J. A. Pople, P. M. W. Gill, B. G. Johnson, *Chem. Phys. Lett.* **1992**, *199*, 557–560.
[53] G. Scalmani, M. J. Frisch, *J. Chem. Phys.* **2010**, *132*, 114110, https://doi.org/10.1063/1.3359469.

Manuscript received: September 12, 2025
Revised manuscript received: September 29, 2025
Version of record online: October 18, 2025